

# Multiplicity and Symmetry Breaking in (Conjectured) Densest Packings of Congruent Circles on a Sphere

James Buddenhagen  
3510 Huntwick Lane, San Antonio TX78230  
e-mail: jbuddenh@texas.net

D. A. Kottwitz  
2152 Hudson Ave, Richland WA 99352  
e-mail: dakc@beta.tricity.wsu.edu

## Abstract

The densest known packing of 15 congruent circles on a sphere occurs in two equally dense varieties. Previously, this was the only known example of a ‘best’ packing of  $n$  circles on a sphere with multiplicity greater than one. We present three new examples:  $n=62$ , 76 and 117. We discuss these and related examples as manifestations of symmetry breaking involving structures we call “rotational toggle hexagons”. Additionally, we present exact data for  $n=15$ , and observe that both the hexagonal packing of the plane and the icosahedral packing of 12 circles on a sphere arise as limiting cases from toggle hexagons.

## 1 Introduction

The problem of packing  $n$  congruent non-overlapping circles on a unit sphere is equivalent to maximizing the minimum distance between any pair of  $n$  points on the sphere (Tammes, 1930 [15]; Fejes Tóth, 1964 [4]). Rigorously proved unique solutions are known only for  $n \leq 14$  and  $n=24$ .<sup>1</sup> For other values of  $n$  various trial-and-error numerical methods have been used to determine dense packings, of which the best known at any epoch are automatically conjectured to be optimal. Large tables of such results, together with many references to earlier work, have been published, most recently by Clare & Kepert 1991 [2] and Kottwitz 1991 [6]. The largest table (extending to  $n=130$ ), created by N. J. A. Sloane, with the collaboration of R. H. Hardin, W. D. Smith and others (1994) and updated as needed, has not been published but is available electronically [5].

By far most of the “best” packings found previously are unique in the sense fully explained below (Section 3). The only exceptional instance is that of  $n=15$ , in which

---

<sup>1</sup> For  $n=13$  and  $n=14$  see Seng-Hwang Lee [7]

there are two distinct packings having circles of exactly equal size (Kottwitz, [6]). Below we shall present three new instances of multiplicity two (for  $n=62, 76$  and  $117$ ) discovered during recent intensive searches. Furthermore every one of these four instances will be shown to result from a type of symmetry breaking based on a characteristic common feature that we call a “rotational hexagonal toggle”, or briefly, a “toggle”. Such features have previously been reported by Leech & Tarnai 1988 [9] in packings of 22 circles that are slightly inferior to the best known. In addition, we shall discuss two already known “best” packings (for  $n=41$  and  $54$ ) in which toggles lead to symmetry breaking without increasing multiplicity. Finally we shall speculate about a slightly different type of toggle that is conceivable but not yet observed in a packing.

It is often convenient to consider the nearer pole of each congruent circle to be a member of a vertex set having a convex hull that is a polyhedron inscribed in the sphere. The length of the circle diameters is equal to the length of the shortest edges of the convex hull, and the number  $N$  of contacts between circles is equal to the number of shortest edges.

## 2 Method

The method used in our recent intensive searches is an elaboration of the repulsion-energy method described previously (Kottwitz, [6]). It should be noted that, while the application of the method to the packing problem was first suggested by Leech in 1957 [8], the basic idea of this least  $p$ -th technique goes back to Pólya (1913) [11]. It is an important algorithm in approximation theory (Rice [12]; Cheney, [1]).

The improvements in the power of our searches are consequences of increases in computer speed, mathematical software capability, and understanding of the problem. There are three chief changes in the previous method (Kottwitz [6]). First, the number of random starts at a moderate value of the exponent  $p$  has been increased from 50 to  $10^5$ , and only a few (3 to 10) of the best first stage results are kept for subsequent escalation of the exponent. The second change is based on the empirical observation that, as the exponent  $p$  increases, the local minima increase in number and occur in closely related clusters. Thus, instead of having a single escalation phase during which an approximate solution is carried straight through from the smallest to the largest exponent  $p$ , we have a set of shorter phases. At the beginning of each escalation phase only the best few earlier results are kept, and each result is several times subjected to a small random perturbation inversely proportional to  $p$ .

The third improvement involves the refinement procedure in which approximate solutions corresponding to  $p$  values of  $10^6$  or higher, are adjusted to “exact” solutions, corresponding to the limit  $p \rightarrow \infty$ . We continue to employ the remarkable empirical fact that (for  $n > 5$ ) each candidate convex hull has been found to have a sufficiently large number of equal shortest edges to provide enough  $(2n - 2)$  independent equations to

determine a unique rigid substructure. This fact is related to Danzer’s “almost conjecture” [3], which has been discussed at length by Tarnai & Gáspár 1983 [16]. The ordinary refinement procedure has been supplemented by a superrefinement that produces as many as 80 significant figures through the use of the variable precision feature of the Maple computer algebra system. When two distinct packings have shortest edges that are equal to such extreme precision, we tentatively conclude that the equality is exact. Since such an equality of irrational numbers is not likely to be an accident but rather the expression of some sort of invariance, we then seek an explanation involving symmetry in some way. Experience so far shows that the explanation is in fact based on symmetry breaking.

### 3 Multiplicity

As mentioned in the introduction, the vast majority of “best” packings are unique, i.e. of multiplicity one. In this we are following a convention in much of mathematics and physics when considering structures in isolation. The difference between right-handed and left-handed versions of a chiral structure is ignored, because it is considered to be essentially trivial.

In order to efficiently recognize possible instances of multiplicity greater than one, the searching process maintains a special list of the top candidate packings. The data for each structure include, in addition to the essential shortest edge length, high-precision values of two invariant quantities  $A$  and  $B$  that have been empirically found to be characteristic of a particular rigid framework (Kottwitz [6]).  $A$  is the average of all distances between vertices of the rigid framework, while  $B$  is the average of the reciprocals of those same distances. The values of  $A$  and  $B$  are independent of the handedness, if any, of the structure. Thus the first indication of an instance of multiplicity greater than one is an output table having two or more top lines with almost equal shortest edge lengths but differing values of  $A$  and  $B$ . The question of exactness of the equality is then resolved practically by the superrefinement procedure.

### 4 Truly Exact Solutions

One interesting feature of the polyhedra (see section 1) associated with solutions of Tamme’s problem is that they can be positioned so the Cartesian coordinates of their vertices are algebraic numbers. This is because the equality of the squared shortest edges determines a system of polynomial equations over the integers, and the vertex coordinates are an isolated solution of this system. In this section we focus on the algebraic number,  $u$ , which is the inner product of unit vectors determined by the endpoints of any shortest edge. Thus  $u = x_i x_j + y_i y_j + z_i z_j$  where  $(x_i, y_i, z_i)$  and  $(x_j, y_j, z_j)$  are the endpoints of a shortest edge.  $u$  is also the cosine of the minimal separation angle, i.e. the central angle subtending a shortest edge. Since the diameter,  $D$ , of each of the congruent circles equals

the length of the shortest edges,  $u$  is also the cosine of the central angle which subtends the diameter of each circle. The quantities  $u$  and  $D$  are related by the equation  $D^2 = 2 - 2u$  so the minimal polynomial of  $D$  normally has twice the degree of the minimal polynomial for  $u$ . Partly for this reason we seek the minimal polynomial for  $u$  rather than for  $D$ . In addition  $u$  is scale-independent whereas  $D$  depends on the arbitrary choice of sphere radius equal to one.

Conceivably, the equations that determine the vertices could be inconsistent. We have, after all, only an approximate solution given by the numerical coordinates output by our search algorithm. Our belief that the alleged circle packing truly exists is bolstered when we observe, as we do, quadratic convergence of our super refinement algorithm, essentially an arbitrary precision implementation of the Newton-Raphson method using Maple. But ultimate confirmation comes from an algebraic solution as provided by a Gröbner basis culminating in a univariate polynomial for  $u$ . This provides, in essence, a description of all coordinates of the polynomial in terms of  $u$ . We were able to find such Gröbner bases using Maple V release 4 in many of the simpler cases.<sup>2</sup> The Gröbner bases are too complicated to present here, but we provide in Table 1 all minimal polynomials for  $u$  that we have been able to compute, together with the associated numeric values of  $u$  accurate to 20 significant figures. These minimal polynomials are for  $u$  when  $n \leq 18$  and when  $n = 20, 24, 27, 30, 32, 38, 48, 50, 52, 120$ . Additional comments follow the table.

**Table 1**

$n$	$u$ (20 digit accuracy)	minimal polynomial for $u$
2	-1.00000000000000000000	$u + 1$
3	-.50000000000000000000	$2u + 1$
4	-.33333333333333333333	$3u + 1$
5	.00000000000000000000	$u$
6	.00000000000000000000	$u$
7	.21013831273060308487	$3u^3 - 9u^2 - 3u + 1$
8	.26120387496374144251	$7u^2 + 2u - 1$
9	.33333333333333333333	$3u - 1$
10	.40439432521625075685	$7u^3 - 4u^2 - 2u + 1$
11	.44721359549995793928	$5u^2 - 1$
12	.44721359549995793928	$5u^2 - 1$
13	.54263648682963846368	$u^8 - 24u^7 - 12u^6 + 8u^5 + 38u^4 + 24u^3 - 12u^2 - 8u + 1$
14	.56395030036050516749	$4u^4 - 2u^3 + 3u^2 - 1$
15	.59260590292507377810	$13u^5 - u^4 + 6u^3 + 2u^2 - 3u - 1$
16	.61229461648269661601	$23u^6 + 6u^5 + 5u^4 + 4u^3 - 3u^2 - 2u - 1$
17	.62809441507002164643	$4u^{10} - 92u^9 + 24u^8 + 128u^7 - 58u^6 - 78u^5 + 35u^4 + 32u^3 - 4u^2 - 6u - 1$
18	.64869583222311652908	$216u^{11} + 108u^{10} + 118u^9 + 209u^8 - 100u^7 - 160u^6 + 40u^5 + 46u^4 - 20u^3 - 12u^2 + 2u + 1$

<sup>2</sup> Unfortunately later releases of Maple contain new Gröbner routines which are ineffective for these problems.

20	.67647713812965145207	$21u^3 - 9u^2 - 5u + 1$
24	.72307846833350853703	$7u^3 + u^2 - 3u - 1$
27	.75838921077657748391	$16u^{24} - 128u^{23} + 536u^{22} - 2088u^{21} + 4977u^{20} - 12258u^{19}$ $+ 20672u^{18} - 36126u^{17} + 51043u^{16} - 73408u^{15} + 104128u^{14}$ $- 137928u^{13} + 175090u^{12} - 181700u^{11} + 155936u^{10}$ $- 92916u^9 + 32222u^8 + 6608u^7 - 16568u^6 + 8192u^5$ $- 1843u^4 - 490u^3 + 128u^2 + 2u - 1$
30	.78155187509498732710	$21508124014u^{29} + 32054106929u^{28} - 17306462662u^{27}$ $- 25038151480u^{26} + 45587477052u^{25} + 38755887413u^{24}$ $- 43255133604u^{23} - 45501640088u^{22} + 10460524458u^{21}$ $+ 17929512405u^{20} - 4828786226u^{19} - 5447284224u^{18}$ $+ 4496890016u^{17} + 4235161545u^{16} - 436447576u^{15}$ $- 1539874224u^{14} - 487336414u^{13} + 100621747u^{12}$ $+ 97938998u^{11} + 20609352u^{10} + 665516u^9 + 320703u^8$ $+ 272188u^7 - 6712u^6 - 34298u^5 - 7289u^4 + 386u^3$ $+ 368u^2 + 56u + 3$
32	.79361661487126244036	$6561u^{22} - 4374u^{21} - 94041u^{20} + 1289844u^{19} + 3605067u^{18}$ $- 4301046u^{17} + 6019389u^{16} + 238896u^{15} - 10407366u^{14}$ $+ 7894164u^{13} + 7975830u^{12} - 7790088u^{11} - 3481466u^{10}$ $+ 3831332u^9 + 843658u^8 - 1303376u^7 - 311819u^6$ $+ 148290u^5 + 39667u^4 - 3660u^3 - 1185u^2 + 18u + 9$
38	.82658325942170668123	$363u^{14} + 7685u^{12} + 34299u^{10} - 77139u^8 + 68985u^6$ $- 31833u^4 + 6561u^2 - 729$
48	.85929229507565992163	$34u^5 + 15u^4 - 12u^3 - 14u^2 - 6u - 1$
50	.86817320912689745167	$386u^{12} + 1679u^{11} + 6433u^{10} - 743u^9 - 2287u^8 - 19290u^7$ $+ 8490u^6 + 19170u^5 - 5580u^4 - 6885u^3 - 1755u^2$ $+ 2997u - 567$
52	.87296670878017463991	$448001u^{16} + 1243448u^{15} + 2260200u^{14} + 2517944u^{13}$ $+ 1365340u^{12} - 424904u^{11} - 1782664u^{10} - 1847944u^9$ $- 864186u^8 - 12568u^7 + 192280u^6 + 95976u^5 + 19676u^4$ $+ 936u^3 - 248u^2 - 24u + 1$
120	.94366230733258023900	$1364u^{10} + 1230u^9 - 709u^8 - 1468u^7 - 688u^6 + 136u^5$ $+ 286u^4 + 108u^3 + 4u^2 - 6u - 1$

For each positive integer  $n \leq 14$  and for  $n = 24$ , table 1 gives the minimal polynomial associated with the proven optimal packing of  $n$  equal circles on a sphere, or in an

alternate parlance, the minimal polynomials associated with the proven optimal spherical codes of size  $n$ . For the other values of  $n$ , the minimal polynomial is for the *conjecturally* optimal spherical code of size  $n$ . For the smallest values of  $n$ , and for the classical cases  $n = 4$  (regular tetrahedron),  $n = 6$  (regular octahedron), and  $n = 12$  (regular icosahedron) it must be considered that these polynomials are well known. However, the only one of these polynomials we have actually seen in print is for  $n = 8$  (square antiprism), and we find this polynomial explicitly in Schütte and van der Waerden [14]. In the same paper they not only prove the optimality for the point arrangements with  $n = 5, 6, 7, 8$ , or 9 points, but also provide sufficient information to easily compute the minimal polynomial for  $u$  for these values of  $n$  and for  $n = 10$  and 24. For example, they state that the radius,  $\rho$ , of the smallest sphere on which 10 points must have pairwise linear separation of at least one unit satisfies the polynomial equation

$$16\rho^6 - 44\rho^4 + 34\rho^2 - 7 = 0.$$

We easily find that  $\rho^2 = 1/(2-2u)$  and, after substituting this into the above polynomial and simplifying, the left side becomes a rational function with numerator  $7u^3 - 4u^2 - 2u + 1$ , our minimal polynomial for  $n = 10$ .

The polynomials in Table 1 of degree 11 or less were found using Gröbner basis methods or resultants in Maple V release 4. The polynomials of degree 12 or more were found using the well known LLL algorithm [10] with superrefined inputs with accuracy from one hundred to several hundred digits. The resulting polynomials were ‘verified’ by computing twice as many digits for  $u$  from the polynomial system, using our super refinement (Newton-Raphson) method, and verifying that when these values are substituted into the alleged minimal polynomials the errors are reduced correspondingly.

The minimal polynomial of  $u$  factors over  $\mathbf{Q}(\sqrt{2})$  for  $n = 8, 16$ ; the minimal polynomial for  $u$  factors over  $\mathbf{Q}(\sqrt{3})$  for  $n = 38$ ; the minimal polynomial for  $u$  factors over  $\mathbf{Q}(\sqrt{5})$  for  $n = 11, 12, 120$ ; the minimal polynomial for  $u$  factors over  $\mathbf{Q}$  extended by the ninth roots of unity when  $n = 7$ . Schütte and van der Waerden [14] give the exact value

$$u = \frac{\cos 80^\circ}{1 - \cos 80^\circ}$$

when  $n = 7$ , and this is easily verified by substituting into  $3u^3 - 9u^2 - 3u + 1$ , the minimal polynomial when  $n = 7$ . Perhaps the easiest way to describe  $u$  when  $n = 7$  is to let  $\tau$  be the root of  $3\tau^3 - 3\tau + 1$  whose approximate value is  $\tau \approx .394931$ . Then the circle diameter squared is  $D^2 = 4\tau$  and  $u = 1 - 2\tau \approx .210138$ .

The remainder of this section is devoted to providing exact coordinates for the polyhedron associated with the packing of 15 equal circles on a unit sphere. This is the least complicated instance of multiplicity greater than one and the only one for which we have been able to present exact coordinates, or even compute a minimal polynomial.

Both of the equally optimal polyhedra for  $n = 15$  have a top consisting of an equilateral triangle from which three equilateral triangular flaps hang down, and a similar bottom although now the flaps point upwards. This accounts for 12 of the 18 vertices shown in Figure 1, where the top and bottom are transparent and each has 3 more triangles attached, ending in the top and bottom pairs  $P, Q$  and  $I, J$  and  $A, B$ . Note that the bottom is rotated a bit with respect to the top. This accounts for 18 vertices in all.

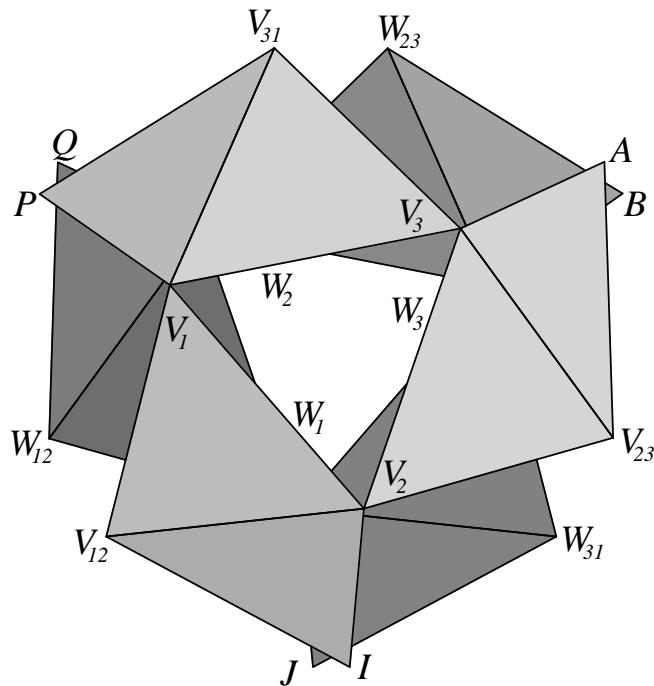


**Figure 1**

The reason there are 18 points instead of 15 is that we hope to lengthen all edges a bit and rotate the top with respect to the bottom a little to make  $P$  coincide with  $Q$  and  $I$  coincide with  $J$  and  $A$  coincide with  $B$  on the equator, thereby reducing the total number of vertices by 3. Unfortunately, however, this causes the points  $V_{12}$  and  $W_{12}$  to be too close to each other (closer than the length of the triangle edges), and similarly for the pairs  $V_{23}, W_{31}$  and  $V_{31}, W_{23}$ , and hence this cannot possibly be an optimal arrangement. The solution is to leave the pairs  $P, Q$  and  $I, J$  and  $A, B$  as 6 separate points, but eventually throw away one point from each pair. This will again reduce the total number of points from 18 to 15. First we use up one of the two degrees of freedom by rotating the top with respect to the bottom until  $W_{12}$  is equidistant from  $P$  and  $V_{12}$ . By the dihedral symmetry of the 18 points, this causes  $W_{31}$  to be equidistant from  $I$  and  $V_{23}$ , and  $W_{23}$  to be equidistant from  $A$  and  $V_{31}$ , and the same for  $V_{12}$  to  $J$  and  $W_{12}, V_{23}$  to  $B$  and  $W_{31}$ , and  $V_{31}$  to  $Q$  and  $W_{23}$ . These edges are all equal in length but may be shorter or longer than the triangle edges.

We use up the other degree of freedom by adjusting the triangle edges until all of these edges are equal, which also makes their common length a maximum.

Now, concerning the proximate point pairs,  $(P, Q)$ ,  $(I, J)$ ,  $(A, B)$ , the first of each pair lies above the equator and the second below. If we remove one point from each pair (and the incident edges) what remains is still a rigid structure but now with only 15 points. There are two possibilities: either the removed points all lie on one side of the equator, or two are on one side and one on the other. In the first case the dihedral symmetry is broken and reduced to a threefold rotational symmetry. In the second case the dihedral symmetry is broken completely and the resulting object has no symmetry. These two structures are the two putatively optimal arrangements for 15 points on a sphere, and clearly they have identical shortest edges.

Figures 2a and 2b show planar maps of these two structures. These were obtained by projecting the structures onto an equatorially tangent cylinder and unrolling it. The left and right sides should be identified in each figure. All solid lines represent shortest edges, 30 for each structure. The dashed lines and the small empty circles they connect represent the removed edges and points.

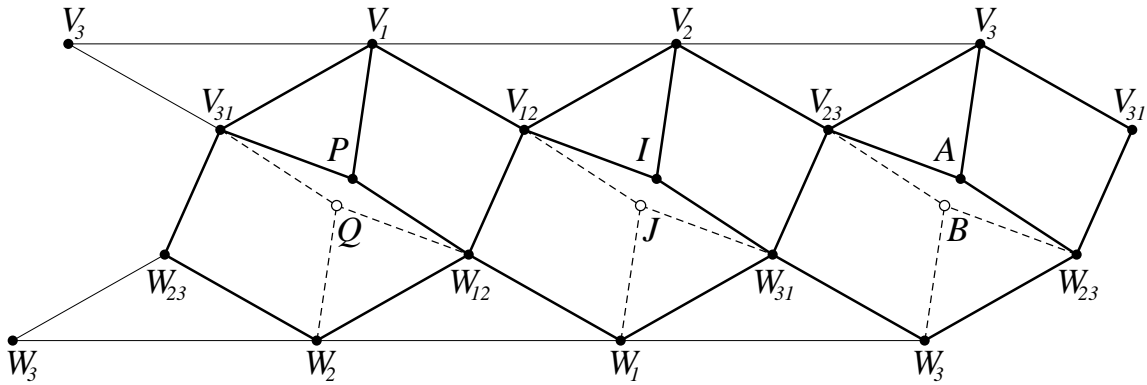


**Figure 2a**

$n = 15$  threefold rotational symmetry



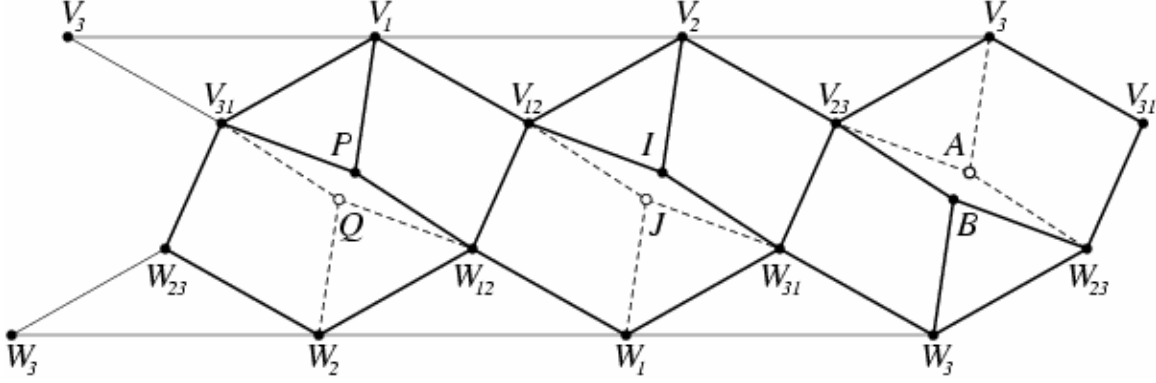


**Figure 2b**

$n = 15$  no symmetry

Note the rotationally symmetric hexagons with two alternative locations for points within. The presence of such hexagons is a repeating theme which will recur in all of the point arrangements discussed in subsequent sections.

Now we give exact coordinates for the 18 points described in the two arrangements for  $n = 15$ . To take advantage of the threefold symmetry axis in the configuration of 18 points we position the centers of the top and bottom triangles on the line  $x = y = z$ , and place the sphere center at the origin. The coordinates then take the form:

$$\begin{array}{lll}
 V_1, V_2, V_3: & (a, b, c), & (c, a, b), & (b, c, a) \\
 V_{12}, V_{23}, V_{31}: & (d, e, f), & (f, d, e), & (e, f, d) \\
 P, I, A: & (r, s, t), & (t, r, s), & (s, t, r) \\
 Q, J, B: & (-t, -s, -r), & (-r, -t, -s), & (-s, -r, -t) \\
 W_{12}, W_{23}, W_{31}: & (-f, -e, -d), & (-e, -d, -f), & (-d, -f, -e) \\
 W_1, W_2, W_3: & (-c, -b, -a), & (-b, -a, -c), & (-a, -c, -b)
 \end{array}$$

All quantities will be expressed in terms of the numbers  $a, b, c$  and  $u$  which must satisfy the constraints  $a^2 + b^2 + c^2 = 1$  and  $ac + ba + cb = u$ . The first equation indicates that  $V_1$  is a unit vector, and the second indicates that the cosine of the minimal separation angle, e.g. the inner product of  $V_1$  and  $V_2$ , equals the number  $u$ . The numeric values of  $a, b, c$ , and  $u$  will be determined later. Details of the computations are omitted but may be checked, most easily with the aid of a computer algebra system. For  $d, e$ , and  $f$  we obtain

$$d = \frac{(2a - b + 2c)u - b}{u + 1}, \quad e = \frac{(2a + 2b - c)u - c}{u + 1}, \quad f = \frac{(-a + 2b + 2c)u - a}{u + 1},$$

and for  $r, s, t$  we obtain

$$r = \frac{(6a - 2c + 3b)u^2 + 2(a - b - c)u - b}{(u + 1)^2}$$

$$s = \frac{(6b - 2a + 3c)u^2 + 2(b - c - a)u - c}{(u + 1)^2}$$

$$t = \frac{(6c - 2b + 3a)u^2 + 2(c - a - b)u - a}{(u + 1)^2}.$$

With these values all 18 vectors will be unit vectors, and all inner products between unit vectors pointing to endpoints of *triangle* edges in Figure 2a (or Figure 2b) will be equal to  $u$ . This is true irrespective of the numeric values of  $a$ ,  $b$ ,  $c$  and  $u$ , providing only that the constraint equations are true and  $u \neq -1$ .

To determine the values of  $a$ ,  $b$ ,  $c$ , and  $u$  which give the optimal structures for  $n = 15$ , we must symbolically solve a system of four simultaneous quadratic equations consisting of the two inner product equations  $W_{12} \cdot P = V_{12} \cdot P = u$  (representative of *non-triangle* edges) together with the constraint equations (see the discussion immediately following Figure 1). The results can be verified using Gröbner basis or other elimination methods in most computer algebra systems. We find that  $u$  satisfies the univariate polynomial equation (its minimal polynomial)

$$13u^5 - u^4 + 6u^3 + 2u^2 - 3u - 1 = 0,$$

and has the approximate numeric value  $u = .592605902925073778$ . From this we find  $b$  using the equation

$$9(4u^2 - u - 1)(3u + 1)^2 b^4 + 2u(62u^4 - 155u^3 - 37u^2 + 51u + 15)b^2 + u^2(4u^2 - u - 1)(5u - 1)^2 = 0,$$

which is a quadratic equation in  $b^2$ . Its roots are approximately  $b_1 = .1714903098093749756$ ,  $b_2 = .814007151904509920$  and their negatives. The equation

$$c = \frac{b(27b^2u^2 + 18b^2u + 29u^3 + 3b^2 - 18u^2 - 11u)}{(3u + 1)(9b^2u + 3b^2 - 5u^2 + u)}$$

gives  $c_1 = .4117319140228847856$ ,  $c_2 = .5737655476910001097$ , and the negatives of these using the four possible substitutions of  $b$ . Finally, substituting  $b = b_1$  and  $c = c_1$  or  $b = b_2$  and  $c = c_2$  into the equation

$$a = \frac{u - bc}{b + c}$$

we get two solutions  $a_1 = .895023968738567582$  and  $a_2 = .090473492975317313$  for  $a$ . Although it appears that we have four solutions,  $u$  as obtained above, together with one of  $(a_1, b_1, c_1)$ ,  $(a_2, b_2, c_2)$ ,  $(-a_1, -b_1, -c_1)$  or  $(-a_2, -b_2, -c_2)$ , in fact these all give the same arrangement of 18 points on a sphere up to orthogonal matrices. Specifically, passing

from  $(a_1, b_1, c_1)$  to  $(a_2, b_2, c_2)$  simply rotates the structure by  $180^\circ$  about the line  $x = y = z$ . In fact, one can show that the matrix equation

$$\frac{1}{3} \begin{pmatrix} -1 & 2 & 2 \\ 2 & -1 & 2 \\ 2 & 2 & -1 \end{pmatrix} \begin{pmatrix} a_1 \\ b_1 \\ c_1 \end{pmatrix} = \begin{pmatrix} a_2 \\ b_2 \\ c_2 \end{pmatrix}$$

is exact. Also, the structures associated with  $(a_1, b_1, c_1)$  and  $(-a_1, -b_1, -c_1)$  are identical except they are of opposite chirality. The same is true for  $(a_2, b_2, c_2)$  and  $(-a_2, -b_2, -c_2)$ .

So there is really just one structure. A couple more facts about it: if  $\beta$  is the angle of rotation between the top and bottom triangles as measured by the angle between the vectors  $W_3 - W_1$  and  $V_2 - V_1$  then

$$\cos \beta = \frac{1-3u}{1+3u} \approx 0.1400052,$$

so  $\beta \approx 98.0481^\circ$ . We might be more likely to consider the offset angle between the top and bottom triangles as  $120^\circ - \beta \approx 21.95185^\circ$ . The angle between the proximate points, that is, between  $P$  and  $Q$  or between  $I$  and  $J$  or between  $A$  and  $B$  is approximately  $12.34265^\circ$ .

This arrangement of 18 points is not a good one because of the pairs  $(P, Q)$ ,  $(I, J)$ , and  $(A, B)$  of close-together points. But, by removing one point from each pair, which can be done in two geometrically different ways, we obtain the two equally optimal but geometrically different arrangements of 15 points on a sphere. This, however, comes at the cost of breaking the symmetry of the original structure.

## 5 Symmetry Breaking

An informal definition might read as follows: symmetry breaking occurs if and only if a symmetrical antecedent structure is followed, logically or temporally, by a less symmetrical consequent structure. A large general class of examples is that in which a governing equation or system of equations has a solution less symmetrical than the equation(s) (Sattinger 1980 [13]). For these the symmetry breaking is said to be spontaneous. Another large class is that of phase transitions, in which a mathematical or material system experiences an abrupt reduction of symmetry when a parameter crosses a critical value. For these the symmetry breaking is said to be induced. In most cases the symmetry group of the consequent structure is a subgroup of the antecedent group. Perhaps this technical condition ought to be added to the definition.<sup>3</sup> A frequent accompaniment of symmetry breaking is an increase in the number of consequent

---

<sup>3</sup> A systematic scholarly account of symmetry breaking and its multitude of manifestations in the arts and sciences is long overdue.

structures. Thus in many nonlinear systems a single stable solution branches into two or more stable solutions at a bifurcation (Sattinger [13]).

In the context of dense packings of congruent circles on a sphere we find that symmetry breaking is manifested in the existence of structures that are very nearly symmetrical. Such structures have much replication of distances between vertices. Thus a table of the frequency of intervertex distance values is a very reliable tool for recognizing symmetry breaking in a single structure. An additional clue pointing toward symmetry breaking is a small excess in the number of shortest edges above the minimum value of  $2n - 2$ .

## 6 Symmetry Breaking With Multiplicity One

In order to introduce symmetrical hexagonal toggles in the simplest possible contexts, we first describe two structures in which symmetry breaking occurs but fails to produce multiple packings.

The first is the ‘best’ packing for  $n=41$ , an old structure in which symmetry breaking was noticed, but the toggle feature was not (Kottwitz [6]). The structure as a whole has no symmetry; however, a subset of 40 vertices constitutes a rigid substructure with a twofold axis of rotation (point group  $C_2$  in Schoenflies notation). Thus  $C_2$  is the antecedent symmetry group in this instance. The odd 41st vertex lies very close to the rotation axis. The structure can be oriented to make this axis vertical with the odd vertex close to the north pole. An orthographic projection of the congruent circles in that neighborhood is shown in Figure 3.

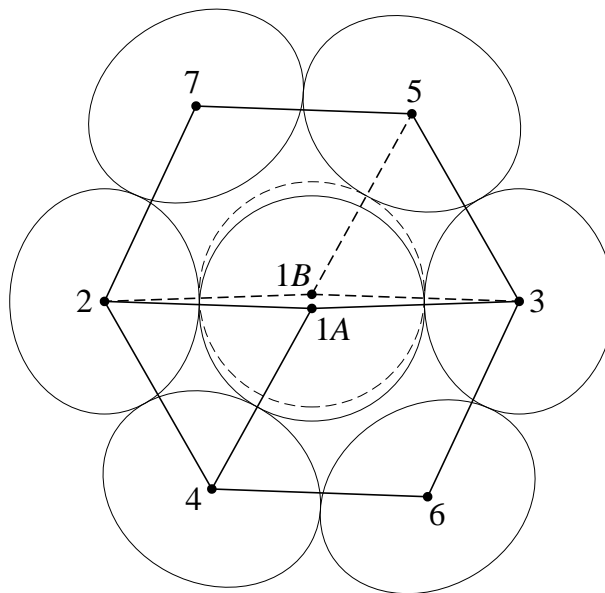


**Figure 3**

Schematic diagram of toggle for  $n=41$ .

Note the distortion due to flattening; on the spherical surface all of the circles are congruent and all segments represent equal arcs of great circles. The odd circle, centered at vertex  $1A$  about  $1.05^\circ$  from the north pole, is surrounded by a ring of six tangent circles in a distorted hexagonal pattern. The odd circle is locked into position by its contacts with circles 2, 3 and 4. Since the ring consists of three symmetrically arranged pairs of circles, it possesses twofold rotational symmetry around the north pole. This symmetry and the finite offset of vertex  $1A$  from the north pole guarantees that there is an alternative site for a vertex at  $1B$ . It is not an additional site, since the circles at  $1A$  and  $1B$  would overlap. A circle (shown by a dotted line) at  $1B$  would be locked by contacts with circles 2, 3 and 5. Now let us imagine that we have begun construction of the complete packing by placing 40 of the circles in all of the twofold symmetrical positions (not shown). Then for the final placement we must choose between  $1A$  and  $1B$ , thus breaking the symmetry. At first sight, it might seem that we can create two distinct structures. However, we soon realize that we would only have two representations of the same structure, rotated  $180^\circ$  with respect to each other. Thus we have symmetry breaking but no increase in multiplicity.

It must be emphasized that the two alternative vertex sites are well defined points. Thus any motion between them would have the nature of a snap action. It is this resemblance to a toggle switch that has led us to dub the seven-circle structure in Figure 3 a “rotational hexagonal toggle” or “toggle” for short.

The second instance of symmetry breaking with multiplicity one occurs for  $n=54$ , again an old structure in which symmetry breaking was noticed, but the toggle features were not (Kottwitz [6]). The whole structure has no symmetry; but a subset of 52 vertices constitutes a rigid substructure having a fourfold rotation-reflection axis (antecedent group  $S_4$ ). When the structure is oriented to have its symmetry axis vertical, there is a toggle at the north pole and an identical one at the south pole. In accordance with  $S_4$  symmetry the two toggles are shifted  $90^\circ$  with respect to each other. The situation is shown schematically in Figure 4, where only the two pairs of potential sites ( $A$  &  $B$ ;  $I$  &  $J$ ) for toggling vertices are shown. Placed at alternating corners of a long upright parallelepiped with a square cross section they directly indicate the symmetry of the omitted subset of 52 vertices. Since each of these pairs is very close ( $0.04^\circ$ ) to the north or south pole, only one member of each can be occupied by a vertex. There are four possible combinations of these vertices:  $AI$ ,  $BJ$ ,  $AJ$  and  $BI$ . It is easy to see that  $AI$  and  $BJ$  give rotated versions of precisely the same structure, as do  $AJ$  and  $BI$ . To get the relationship between  $AI$  and  $AJ$ , we apply the basic symmetry operation (generator) of the group  $S_4$ , which is a rotation of  $90^\circ$  around the vertical  $z$ -axis followed by a reflection in the horizontal  $x, y$ -plane, to the combination  $AI$ . The result is  $AJ$ . This shows that  $AI$  and  $AJ$  are merely rotated mirror images of each other; the same is true for  $BI$  and  $BJ$ . According to the convention adopted in Section 3, right-handed and left-handed versions of a structure are equivalent for purposes of counting multiplicity. Thus, although there is symmetry breaking from the fourfold antecedent group  $S_4$  to the trivial group  $C_1$ , the multiplicity is only one.

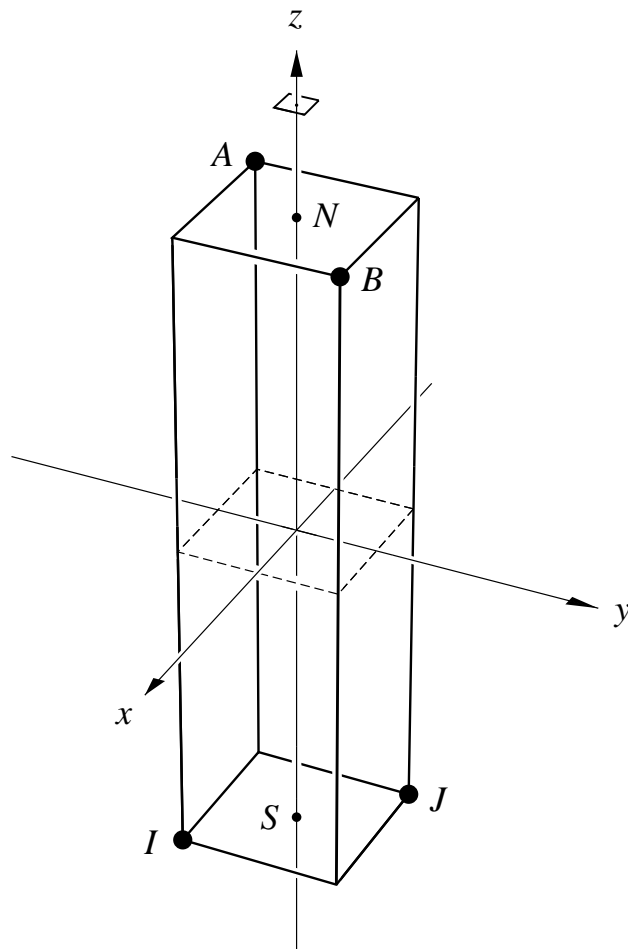


**Figure 4**

Schematic diagram of the two pairs of toggle sites for  $n=54$ .

## 7 Symmetry Breaking With Multiplicity Two

The first instance of symmetry breaking with multiplicity two occurs for  $n=15$ , an old pair in which the toggle features were not previously noticed (Kottwitz [6]). One of the structures has a threefold rotation axis (group  $C_3$ ), and the other has no symmetry. A subset of 12 of the vertices constitutes a rigid substructure having a vertical threefold rotation axis and three horizontal twofold rotation axes (antecedent group  $D_3$  of order 6). Each of the three odd vertices lies inside a rotational hexagonal toggle centered at a horizontal axis. The situation is shown schematically in Figure 5, where only the three pairs of potential toggle sites ( $A$  &  $B$ ;  $I$  &  $J$ ;  $P$  &  $Q$ ) are placed along the edges of a circular band representing an equatorial zone of the sphere. They embody the sixfold symmetry of the omitted subset of 12 vertices. Again only one of each pair of sites may be occupied by a vertex. With two choices at each toggle, there are a total of  $2^3=8$  combinations. However two of these,  $AIP$  and  $BJQ$ , in which all three odd vertices are on the same side of the equator, are rotationally equivalent. So are the other six combinations, in which there is one vertex on one side of the equator and two on the

other. Thus there are only two distinct structures, the first of which has threefold rotational symmetry, while the second has no symmetry.

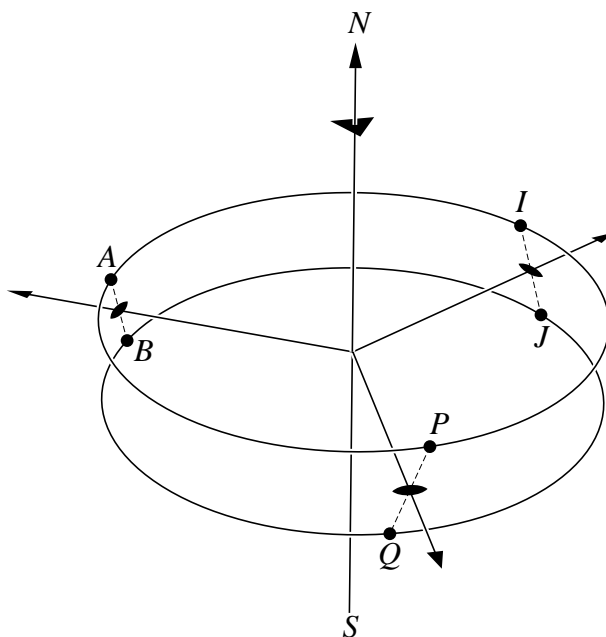


**Figure 5**

Schematic diagram of the three pairs of toggle sites for  $n=15$  and  $n=117$ .

The second instance of multiplicity two occurs for  $n=62$ . One of these structures was discovered previously (Sloane & Hardin [5]), while the other is new. Each of these distinct structures has a single twofold rotation axis (group  $C_2$ ). A subset of 60 of the vertices constitutes a rigid substructure having three orthogonal twofold axes (antecedent group  $D_2$  of order four). Each of the two odd vertices lies inside a rotational toggle centered at opposite ends of one of the horizontal axes. The situation is shown schematically in Figure 6, in which only the two pairs of potential toggle sites ( $A$  &  $B$ ;  $I$  &  $J$ ) are placed at alternate corners of a long thin rectangular parallelepiped. They directly indicate the symmetry of the omitted subset of 60 vertices. Since each of these pairs is very close (about  $0.9^\circ$  to the rotation axis ( $x$ -axis)), only one member of each can be occupied by an odd vertex. There are  $2^2=4$  possible combinations:  $AI$ ,  $BJ$ ,  $AJ$  and  $BI$ .  $AI$  and  $BJ$  give the same structure, and  $AJ$  and  $BI$  give another one. Thus there are only two distinct structures, each having twofold rotational symmetry ( $C_2$ ).

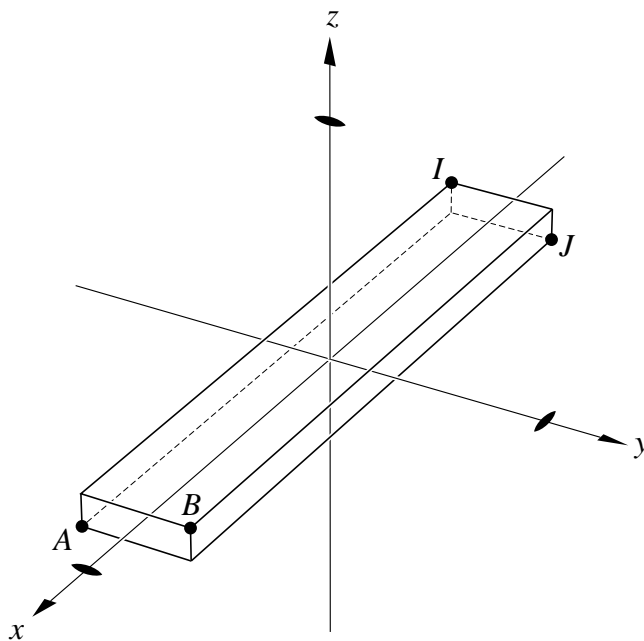


**Figure 6**

Schematic diagram of the two pairs of toggle sites for  $n=62$  and  $n=76$ .

The third instance of multiplicity two occurs for  $n=76$ . Again one of these structures was found previously (Sloane and Hardin, [5]), and the other is new. There is a great resemblance between this pair of structures and the pair for  $n=62$  discussed above. The schematic diagram in Figure 6 is still applicable. The major difference is that these structures have 74 vertices in the omitted subset having unbroken antecedent  $D_2$  symmetry, including two located on the  $y$ -axis. This accounts for the fact that this number (74) is not a multiple of 4. Again there are two distinct structures, each having twofold rotational symmetry ( $C_2$ ).

The fourth instance of multiplicity two occurs for  $n=117$ . One of these structures was found previously (Sloane & Hardin [5]), and the other is new. This pair bears a great resemblance to the pair for  $n=15$ . The diagram in Figure 5 is applicable. Thus there are two distinct structures, one having threefold rotational symmetry ( $C_3$ ) and the other having no symmetry.

## 8 Summary of Results

A summary of the symmetry-related properties of the packings that exhibit symmetry breaking is given in Table 1. For each value of  $n$  the following items are listed: the Schoenflies symbol  $G$  of the point group; an indication  $E$  (Yes/No) whether or not the structure is chiral; the order  $O$  of the point group; the number  $T$  of toggle features; the multiplicity  $M$ ; a list of  $s_i(m_i)$  for the number  $s_i$  of subsets containing  $m_i$  equivalent vertices; the Schoenflies symbol  $G_A$  of the antecedent point group; the order  $O_A$  of the



antecedent point group; and a literature reference. Several of these items, as well as most of those in the following Table 2, have been described in detail previously (Kottwitz, [6]).

Table 1

$n$	$G$	$E$	$O$	$T$	$M$	$s_i(m_i)$	$G_A$	$O_A$	Reference
15A	$C_3$	Y	3	3	2	5(3)	$D_3$	6	Schütte & van der Waerden (1951), [12]
15B	$C_1$	Y	1	3	2	15(1)	$D_3$	6	Kottwitz (1991), [6]
41	$C_1$	Y	1	1	1	41(1)	$C_2$	2	Kottwitz (1991), [6]
54	$C_1$	Y	1	2	1	54(1)	$S_4$	4	Kottwitz (1991), [6]
62A	$C_2$	Y	2	2	2	31(2)	$D_2$	4	Hardin, Sloane & Smith (1994), [5]
62B	$C_2$	Y	2	2	2	62(1)	$D_2$	4	Present work (found in 1994)
76A	$C_2$	Y	2	2	2	37(2),2(1)	$D_2$	4	Hardin, Sloane & Smith (1994), [5]
76B	$C_2$	Y	2	2	2	38(2)	$D_2$	4	Present work (found in 1994)
117A	$C_3$	Y	3	3	2	39(3)	$D_3$	6	Present work (found in 1994)
117B	$C_1$	Y	1	3	2	117(1)	$D_3$	6	Hardin, Sloane & Smith (1994), [5]

A summary of the metric properties of these packings is given in Table 2. The following items are listed there: the linear diameter  $D$  of the congruent circles; the number  $N$  of shortest edges (circle contacts); the average distance  $A$  between vertices of the rigid framework; the average  $B$  of the reciprocal of the distance between vertices of the rigid framework; the angular diameter  $d$  in degrees of the congruent circles; the packing density  $F$ ; the number  $R$  of vertices free to rattle; the number  $H$  of holes (which contain rattlers); and the central angle  $t$  in degrees between the toggle positions.

Table 2

$n$	$D$	$N$	$A$	$B$	$d^\circ$	$F$	$R$	$H$	$t^\circ$
15A	0.90265618822997	30	1.412540888198	0.769991232589	53.657850129933	0.807314364191	0	0	12.342651435515
15B	0.90265618822997	30	1.412675682176	0.769957408268	53.657850129933	0.807314364191	0	0	12.342651435515
41	0.56349562016289	81	1.363408493292	0.849150683902	32.729094415061	0.830485858088	0	0	2.109406749588
54	0.49597518817382	106	1.356382579540	0.866351797858	28.716920529594	0.843393383937	0	0	0.086763877870
62A	0.46152605437000	124	1.353475945172	0.874443591227	26.683996996404	0.836690554611	0	0	1.714721258402
62B	0.46152605437000	124	1.353475918465	0.874443597904	26.683996996404	0.836690554611	0	0	1.714721258402
76A	0.41801164317790	150	1.350104107031	0.885249889189	24.128194441650	0.839252939607	2	2	1.039201778830
76B	0.41801164317790	150	1.350104096591	0.885249891799	24.128194441650	0.839252939607	2	2	1.039201778830
117A	0.33803314892755	225	1.344344359790	0.906792209051	19.461291100101	0.841627279398	6	3	0.064529442388
117B	0.33803314892755	225	1.344344359764	0.906792209073	19.461291100101	0.841627279398	6	3	0.064529442388

Detailed numerical results for each packing are available electronically.<sup>4</sup> The items tabulated include coordinates for each vertex.

<sup>4</sup> The Internet address is <http://jbuddenh.home.texas.net/pack/sphere/mult/>

## 9 Discussion

The single feature common to all of the observed instances of symmetry breaking is the rotational hexagonal toggle sketched in Figure 3. Each of these toggles is centered at a twofold rotation axis of a substructure that contains a great majority of the vertices. The presence of a vertex at one of the toggle sites destroys the antecedent rotational symmetry operation, thus reducing the symmetry of the complete structure.

If only one toggle feature is present, as for  $n=41$ , symmetry breaking occurs, but multiplicity is not increased. If there are two toggles, the situation is more complicated; for  $n=54$  multiplicity is not increased, but for both  $n=62$  and  $n=76$  the multiplicity is two. Finally for both  $n=15$  and  $n=117$ , where the number of toggles is three, the multiplicity is two.

The toggles represented schematically by Figure 3 differ in size and shape. In fact these toggles have two degrees of freedom. A natural pair of descriptive parameters would be the angular diameter  $d$  of the congruent circles and the arc length between the alternative vertex sites  $1A$  and  $1B$ .

## 10 Hypothetical Structures With Symmetry Breaking

In addition to those already observed it is easy to imagine other types of structures having symmetry breaking and multiplicity greater than one. The simplest would have an antecedent point group  $C_2$  (a single twofold axis) and a toggle centered at each pole. The consequent structures would have multiplicity two and no symmetry.

A more general class of structures might have an antecedent point group  $D_j$ , where  $j > 3$ . This has a  $j$ -fold vertical axis and  $j$  twofold horizontal axes. There would be a toggle centered at one pole of each horizontal axis. For example, for  $j = 4$ , there would be  $2^4 = 16$  possible combinations of toggle settings eventually resulting in a multiplicity of four. In fact, a packing in this class was described a decade ago, but since it was found to be suboptimal and unstable, it was mentioned only in passing (Leech & Tarnai [9]).

A different class of structures could result from a hypothetical variety of toggle feature, which is shown schematically in Figure 7. The only difference between Figures 3 and 7 is the positioning of vertices 4 and 6. In Figure 7 the hexagonal ring has reflectional rather than rotational symmetry. Thus we designate the entire hypothetical feature as a "reflectional hexagonal toggle". Such a feature would naturally be centered at a point on a reflection plane. If two or more such features were located at the same reflection plane, then alternative combinations of vertex sites like  $1A$  and  $1B$  would result in symmetry breaking and increased multiplicity.

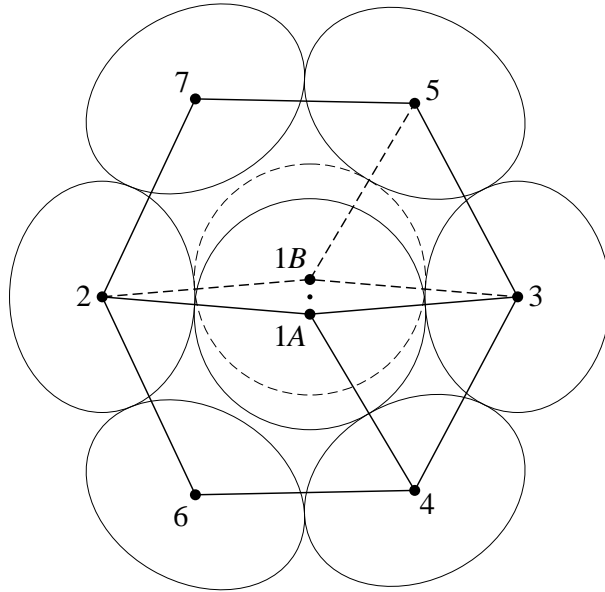


**Figure 7**

Schematic diagram of a hypothetical reflectional hexagonal toggle.

The ultimate variety of hexagonal toggle comes into existence when, for a given circle size, the separation between vertex sites  $1A$  and  $1B$  reaches its maximum value. Then the diagrams in Figures 3 and 7 coalesce into one, and the hexagonal ring has both rotational and reflectional symmetry. Since such a hypersymmetric toggle has only one degree of freedom, it must be a highly improbable instrument for symmetry breaking in very dense packings. Nevertheless, it may be of some interest, since its two limiting cases do in fact occur in two of the most interesting and symmetric densest packings. As the diameter of circles in the hypersymmetric hexagonal toggle decreases to zero, the separation between the vertex sites  $1A$  and  $1B$  decreases to zero. As long as  $1A$  and  $1B$  are distinct, there is a legitimate toggle. At the limit, where  $1A$  and  $1B$  coincide, the toggle feature vanishes, and we are left with only one inner circle in contact with the six congruent circles that form a regular hexagonal ring. This limit corresponds to the hexagonal packing of circles on a plane, known to be the densest possible. At the other extreme, as the separation between  $1A$  and  $1B$  increases to  $d$ , the overlap between the inner circles decreases toward zero. As long as the area of overlap is nonzero, there is a legitimate toggle. At the limit, where the separation is  $d$ , the overlap and the toggle feature vanish simultaneously. Then there is space for an additional inner circle in the packing. Each inner circle is in contact with five congruent circles that form a regular pentagonal ring. This limit corresponds to the regular icosahedral packing of 12 congruent circles on a sphere, known to be a very dense packing. Thus we conclude by noting that the hypothetical hypersymmetric toggle is in some sense a connecting link between the two most remarkable packings known.

## Acknowledgement

It is a pleasure for one of us (D. A. K.) to acknowledge the generous cooperation and assistance of the faculty and staff of Washington State University at Tri-Cities, especially Alyssa M. Dodd and Professor Lee D. Philipp.

## References

- [1] E. W. Cheney, Introduction to approximation theory, McGraw-Hill, NY, 1966.
- [2] B. W. Clare & D. L. Kepert, The optimal packing of circles on a sphere, *J. Math. Chem.* 6 (1991), 325-349.
- [3] L. Danzer, Endliche Punktmengen auf der 2-Sphäre mit möglichst grossem Minimalabstand. Habilitationsschrift, Univ. Göttingen, Germany (1963). English transl: *Discrete Math.* 60 (1986), 3-66.
- [4] L. Fejes Tóth, Regular figures, Pergamon-Macmillan, NY, 1964
- [5] R. H. Hardin, N. J. A. Sloane, W. D. Smith, *et al.* (1994), Tables of Spherical Codes, published electronically at <http://www.research.att.com/~njas/packings/dim3/>
- [6] D. A. Kottwitz, The densest packing of equal circles on a sphere, *Acta Cryst.* A47, (1991), 158-165.
- [7] Seng-Hwang Lee, Arrangements of 13 and 14 points on the unit sphere with maximum minimum distance. Ph.D. dissertation, Univ. of California, Berkeley, California, U.S.A.
- [8] J. Leech, Equilibrium of sets of particles on a sphere, *Math. Gaz.* 41 (1957), 81-90.
- [9] J. Leech & T. Tarnai, Arrangements of 22 circles on a sphere, *Ann. Univ. Sci. Budapest Ser. Math.* 31 (1988), 27-37.
- [10] A. K. Lenstra, H. W. Lenstra and L. Lovász, Factoring polynomials with rational coefficients, *Math. Ann.* 261 (1982), 515-534.
- [11] G. Pólya, Sur un algorithme toujours convergent pour obtenir les polynomes de meilleure approximation de Tchebychef pour une fonction continue quelconque, *Compt. Rend. Acad. Sci.* 157 (1913), 840-843.
- [12] J. R. Rice, The approximation of functions Addison-Wesley, NY, 1964.
- [13] D. H. Sattinger, Bifurcation and symmetry breaking in applied mathematics, *Bull. Amer. Math. Soc. NS.* 3 (1980), 779-819.
- [14] K. Schütte & B. L. van der Waerden, Auf welcher Kugel haben 5, 6, 7, 8 oder 9 Punkte mid Mindestabstand Eins Platz? *Math. Ann.* 123 (1951), 96-124.
- [15] P. M. L. Tammes, On the origin of number and arrangements of the places of exit on the surface of pollen-grains, *Recl. Trav. Bot. Neerl.* 27 (1930), 1-84.
- [16] T. Tarnai & Z. Gáspár, Improved packing of equal circles on a sphere and rigidity of its graph, *Math. Proc. Cambr. Phil. Soc.* 93 (1983), 191-218.